Catalysis Today 170 (2011) 56–63

Contents lists available at ScienceDirect

Catalysis Today

journal homepage: www.elsevier.com/locate/cattod

Review

Catalytic hydrolysis of ammonia borane for chemical hydrogen storage

Hai-Long Jiang, Qiang Xu*

National Institute of Advanced Industrial Science and Technology (AIST), Ikeda, Osaka 563-8577, Japan

ARTICLE INFO

Article history:
Available online 27 October 2010

Keywords:
Ammonia borane
Hydrolysis
Heterogeneous catalysis
Hydrogen storage

ABSTRACT

Hydrogen storage for vehicular applications requires high gravimetric/volumetric storage capacity. Ammonia borane (NH_3BH_3, AB), having hydrogen content as high as 19.6 wt%, has been considered as a highly potential hydrogen storage medium for on-board applications. The AB hydrolytic dehydrogenation system presents a hydrogen capacity up to 7.8 wt% of the starting materials AB and H_2O, showing its high potential for chemical hydrogen storage. With significant research efforts, the reaction kinetics has been greatly enhanced under ambient conditions and the catalyst cost has been remarkably lowered for the hydrolytic dehydrogenation of AB in recent five years. Herein, we briefly review the research progresses in catalytic hydrolytic dehydrogeneration from ammonia borane for chemical hydrogen storage. Moreover, we also concisely discuss hydrogen release from aqueous hydrazine boranes, derivatives of AB, as new hydrogen storage materials.

Contents

1. Introduction

There is an increasing and impending demand for sufficient energy supply along with the continuously growing population and the rising standards of living in the world. Hydrogen, as a globally accepted clean and source-independent energy carrier [1], has a high energy content per mass compared to petroleum (120 MJ kg^{-1} for hydrogen versus 44 MJ kg^{-1} for petroleum) and can be energy sources for different end uses, such as hydrogen fuel cell vehicles and portable electronics.

For transportation applications, the energy carrier is required to have a small volume and mass, as well as high energy content, so that it can be stored in a small space and used in a high efficiency. In order to meet the targets set by the U.S. Department of Energy (US DOE) [2], different storage solutions have been developed and a large number of publications on hydrogen storage materials, such as metal hydrides [3,4], sorbents [5–7], on-board reforming of hydrocarbon into hydrogen [8], and organic materials [9] have been reported, while big challenges still remain.

Chemical storage materials with high hydrogen contents are highly promising as hydrogen sources for fuel cells. Among them, boron- or nitrogen-based compounds, such as, $LiNH_2$–LiH, Li/$NaBH_4$ and N_2H_4, etc., have attracted much attention [10–14]. The simplest B–N compound of ammonia borane (NH_3BH_3, AB), with low molecular weight (30.9 g mol^{-1}) and a hydrogen capacity as high as 19.6 wt%, exceeding those of gasoline and Li/$NaBH_4$, is today the most promising boron hydride for on-board hydrogen storage applications [6,12,15–24].

* Corresponding author. Tel.: +86 72 751 9562; fax: +86 72 751 7942.
E-mail address: q.xu@aist.go.jp (Q. Xu).

0920-5861/$ – see front matter © 2010 Elsevier B.V. All rights reserved.
doi:10.1016/j.cattod.2010.09.019

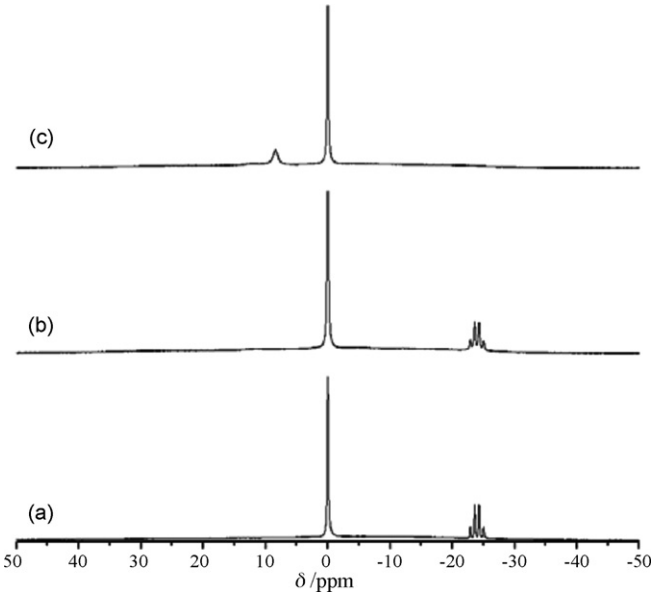

Fig. 1. ^{11}B NMR spectra of (a) aqueous AB solution freshly prepared, (b) after 1 month under Ar atmosphere, and (c) after reaction in the presence of suitable catalyst. The peak at 0 ppm is due to the external reference $BF_3{\cdot}(C_2H_5)_2O$.

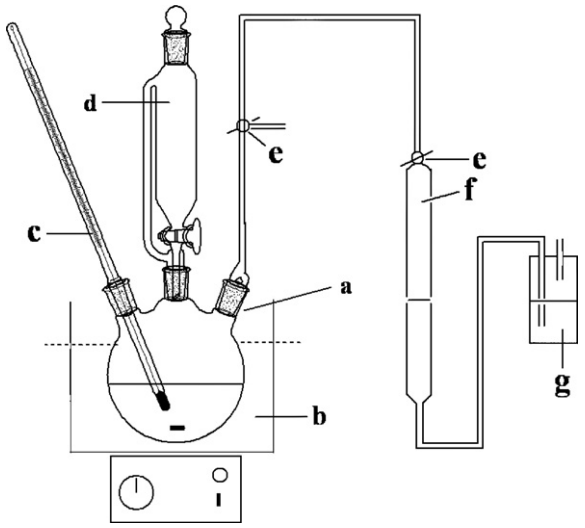

Fig. 2. The reaction apparatus for monitoring hydrogen generation from aq. AB. (a) three-necked flask, (b) water-bath stirrer, (c) thermometer/pH meter, (d) additional funnel with a pressure equalized arm, (e) gas valve, (f) gas burette and (g) reservoir.

Ammonia borane is a colorless molecular crystal with tetragonal structure under ambient conditions and soluble in H_2O and other relatively polar solvents (for example, methanol) [18,22]. Pure AB has a density of 0.74 g cm^{-3} and a melting point of 110–125 °C. It is first synthesized in the mid-1950s for developing boron hydride based high-energy fuels for jets and rockets. Presently, several laboratory-scale preparation methods have also been established and one of the most effective method gives high purity (≥98%) and high yield (≥95%), which involves the reaction of $NaBH_4$ and ammonium formate (HCO_2NH_4) in dioxane [18,25]. Most importantly, AB is nontoxic, stable, environmental benign, and can be safely handled under ambient conditions, which greatly facilitate its application.

To data, considerable works involving the hydrogen release from the thermal dehydrogeneration of AB have been reported [15,16,26–29]. The thermal dehydrogeneration temperature can be lowered in an organic solution or ionic liquid [26]. In contrast to neat AB, the threshold temperature can be reduced and volatile byproducts can be effectively suppressed by loading AB into different scaffolds (such as, SBA-15 [15], CMK-3 [27], and porous metal-organic framework [16]) or doping with Li [27]. In addition, reaction of AB with metal hydrides (such as, LiH, NaH [28], or CaH_2 [29]) yields metal amidoboranes of $M(NH_2BH_3)_n$ (M = Na, n = 1; M = Ca, n = 2), which can release hydrogen at lower temperatures with much lower propensity for borazine formation. Generally speaking, thermal decomposition of AB needs high temperature and power consumption. In contrast, the catalytic hydrolysis provides a more promising method for hydrogen generation from AB. Colorless aqueous solution of AB is highly stable (over 1 month) in an argon atmosphere, exhibiting a quadruplet centered at δ = −23.9 ppm with $^1J_{B-H}$ = 91 Hz in the ^{11}B NMR spectra (Fig. 1) whereas it undergoes very slow hydrolysis reaction in air due to the catalytic activity of carbon dioxide [30,31]. The hydrolysis reaction (Eq. (1)) can be significantly accelerated in the presence of suitable catalysts, as evidenced by the decrease until the disappearance of the ^{11}B peak at −23.9 ppm for aqueous NH_3BH_3 and the appearance of an additional low field-shifted single ^{11}B resonance due to the production of borate species (Fig. 1). Therefore, one of the major obstacles for the practical application of the catalytic hydrolysis dehydrogenation of AB is to develop efficient and economical catalysts to improve the kinetic properties under moderate reaction conditions.

$$NH_3BH_3 + 2H_2O \rightarrow NH_4^+ + BO_2^- + 3H_2 \quad (1)$$

In this review, we briefly survey the research progresses in catalytic hydrogen generation from hydrolysis of AB under ambient conditions in recent five years since the first work was published by our group in 2006 [30].

2. Experimental set-up and procedure

2.1. Experimental set-up

As illustrated in Fig. 2, an experimental apparatus is devised for monitoring the hydrogen generation amount/rate from the AB aqueous solution, which consists of a three-necked round-bottom flask with one of the flask openings connected to a gas burette, one to an addition funnel with a pressure-equalization arm, and the other one to a thermometer or pH meter.

2.2. Experimental procedure

The AB powder is placed in the three-necked flask and the reaction is started by stirring the mixture of the AB and the catalyst aqueous solution added from the additional funnel (for liquid catalysts or catalyst precursors); or the AB powder and catalyst are placed in the flask and distilled water added from the funnel to trigger the reaction (for solid catalysts). The evolution of gas was monitored using the gas burette (the water levels are adjusted to equal height by moving the reservoir during hydrogen evolution). The solution temperature can be controlled by a water-bath stirrer (coolant can be changed with water for cooling if necessary). After the completion of the reaction, the solutions can be filtered to separate the catalyst as residue. The filtrates and the catalyst are used for further characterizations (such as, ^{11}B NMR, powder XRD, TEM, etc.).

3. Catalysts

Through five years of exploration and efforts, it has been found that almost all of active catalysts toward hydrolysis of AB are highly

dependent on metal sites. Herein, we discuss the progresses on hydrolysis of AB on the basis of metal catalyst classification.

3.1. Noble metal-based catalysts

Noble metal-based catalysts were firstly found to have considerable activities toward hydrolytic dehydrogenation of AB. The Pt-based catalysts were firstly reported to have high activity toward this reaction with the released H_2 to AB ratio up to 3.0 and the catalytic activities are in the order of 20 wt% Pt/C > 40 wt% Pt/C > PtO_2 > Pt black > K_2PtCl_4. The 20 wt% Pt/C catalyst shows the superhigh activity and the reaction is completed in less than 2 min. In contrast, Rh[(1,5-COD)(μ-Cl)]$_2$ and Pd black have lower activity and some noble metal oxides (RuO_2, Ag_2O, Au_2O_3, IrO_2) are almost inactive [30]. The activity of cationic Pt-based salts for AB hydrolysis reaction can be ascribed to the reduction of Pt^{n+} (n = 4, 6) to Pt^0 during the course of the reaction, which is supported by TEM observations [30] and X-ray diffraction (PXRD) analyses [32]. The γ-Al_2O_3 and SiO_2 supported Ru, Rh, Pd, Pt and Au nanoparticles (NPs) were also investigated for hydrolysis of AB by our group [33]. It has been found the Ru, Rh and Pt catalysts exhibit high activities to generate stoichiometric amount of hydrogen with fast kinetics, whereas the Pd and Au catalysts are less active. Furthermore, investigations on Pt NPs supported on different supports (γ-Al_2O_3, VULCAN® carbon and SiO_2) reveal the support effects are mostly attributed to the change of particle size, and the hydrogen release rate is not dependent on the AB concentration [33]. Manners and co-workers reported Rh(0) species (e.g., Rh black, Rh stabilized on alumina, aqueous Rh colloids) as active catalysts for hydrolysis of AB and proposed a heterogeneous mechanism [34]. Rhodium NPs were deposited on different supports (γ-Al_2O_3, TiO_2 and carbon) and the activities of these catalysts were different, in which Rh/TiO2 gave the best activity in the hydrolysis of AB although the sizes of Rh NPs formed were similar [35]. It has been reported by Basu et al. that the Ru/C catalyst is active and has an activation energy of 76 ± 0.1 kJ mol^{-1}. The observed hydrogen release rates are 843 ml H_2 min^{-1} (g catalyst)$^{-1}$ and 8327 ml H_2 min^{-1} (g catalyst)$^{-1}$ at 25 °C and 55 °C, respectively [36]. They also investigated the isothermal hydrogen release rate of dilute AB (1 wt%) hydrolysis in the presence of carbon supported ruthenium catalyst (Ru/C) with catalyst particle sizes of 20–181 μm and in a temperature range of 26–56 °C and the results obtained under dilute AB conditions showed an activation energy of 60.4 kJ mol^{-1} [37].

In order to achieve well dispersed noble metal clusters/NPs with small sizes, Özkar and co-workers have recently used different polymers as stabilizers for metal NPs. The water soluble laurate (dodecanoate, $C_{12}H_{23}NaO_2$)-stabilized Rh NPs with an average size of 5.2 ± 2.7 nm were prepared by the reduction of rhodium(III) chloride over dimethylamine–borane in solution containing sodium laurate at room temperature. The laurate-stabilized Rh NPs showed exceptional catalytic activity with a turnover frequency (TOF) value of 200 mol H_2/mol Rh min^{-1} and unprecedented catalytic lifetime with 80,000 turnovers in the hydrolysis of AB in air at 25.0 °C [38]. They have also prepared water dispersible laurate-stabilized Ru NPs with an average size of 2.6 ± 1.2 nm by the same method from $RuCl_3 \cdot 3H_2O$ and found that the laurate-stabilized Ru NPs are highly active and long-life catalyst with a TOF of 75 mol H_2/mol Ru min and total turnover number (TTON) value of 5900 mol H_2/mol Ru in the hydrolysis of AB at 25.0 °C [39]. In addition, the authors used water-soluble poly(4-styrenesulfonic acid-co-maleic acid), PSSA-co-MA, as an alternative stabilizer to prepare Ru NPs and Pd NPs with average particle sizes of 1.9 ± 0.5 nm and 3.5 ± 1.6 nm, respectively, *in situ* from the reduction of $RuCl_3$ and K_2PtCl_4 during the AB hydrolysis reaction at room temperature [40]. It is found that PSSA-*co*-MA stabilized Ru NPs and Pd NPs are highly active and provide 51,720 and 8720 turnovers, respectively, in the hydrogen generation from the hydrolysis of AB at 25 °C before deactivation. The deactivation is probably due to the increasing viscosity of the solution or deactivation effect of increasing metaborate concentration. The activation energies for the hydrolysis of AB in the presence of PSSA-*co*-MA stabilized Ru and Pd NPs are 54 ± 2 kJ mol^{-1} and 44 ± 2 kJ mol^{-1}, respectively. Kinetics studies show that the catalytic hydrolysis of AB is of first order with respect to the catalyst concentration, whereas it is of zero order with respect to the substrate concentration in the case of both Ru and Pd NPs [40]. It is a feasible approach to confine the active metal NPs inside void spaces such as mesoporous or microporous solids for preventing aggregation of metal NPs. Zeolite-Y with highly ordered supercages with a diameter of 1.3 nm was selected as a suitable host for preparing Rh and Pd NPs with small sizes [41–43]. The zeolite-stabilized Rh and Pd NPs were prepared at room temperature by ion-exchange of Rh^{3+} or Pd^{2+} cation with the extra framework Na^+ ions in zeolite-Y, followed by *in situ* reduction of the metal cations during the catalytic hydrolysis of AB (for Rh NPs) or with sodium borohydride in aqueous solution (for Pd NPs). The zeolite-stabilized Rh and Pd NPs are found to be isolable, redispersible, and reusable as an active catalyst in the hydrolysis of AB and provide exceptional catalytic activities (TOF = 92 mol H_2/mol Rh min for Rh NPs) and long lifetime (47,200 turnovers for Rh NPs and 15,600 turnovers for Pd NPs) in the hydrolysis of AB at 25 °C. Moreover, the complete release of hydrogen is achieved even in successive runs performed by redispersing the zeolite-stabilized Rh NPs isolated after the previous run. The authors attributed the outstanding catalytic activity and catalytic lifetime of zeolite-stabilized Rh NPs to the small size and narrow size distribution of the Rh NPs, which are almost half-naked interacting with internal or external surface of zeolite [42,43]. Some reported noble metal-based catalysts for hydrogen generation from aqueous AB are summarized in Table 1.

3.2. Non-noble metal-based catalysts

Although the noble metal-based catalysts show very high activities for hydrolysis of AB as mentioned above, from the viewpoint of practical application, the development of efficient, low-cost, and stable catalysts to further improve the kinetic properties under moderate conditions is therefore very important. Bearing this in mind, we firstly studied catalytic performance of supported non-noble metals for hydrogen generation from aqueous AB at room temperature and found supported Co, Ni and Cu were the most catalytically active under our experimental conditions, with which hydrogen is released with an almost stoichiometric amount from aqueous AB, whereas supported Fe is catalytically inactive for this reaction. Among the different supports (γ-Al_2O_3, SiO_2 and C) for Co NPs, the Co/C catalyst has the highest activity. Similar to those of noble metal NPs, the activity of the supported catalyst is increased with decreasing the particle size of non-noble metal NPs [44]. Afterwards, we systematically investigated the catalytic activities of unsupported first-row transition metal NPs, which were pre-reduced by $NaBH_4$ or *in situ* reduced in the presence of AB and $NaBH_4$ during the hydrolysis reaction. It is found that the catalytic activities are highly dependent on their particle sizes, crystallinities, compositions, etc. [45–50]. In the presence of $NaBH_4$ and NH_3BH_3 as the co-reducing agents, the amorphous Fe NPs were *in situ* formed and showed exceptionally high catalytic activity, with which the hydrolysis reaction was completed within 8 min (metal/AB = 0.12, Fig. 3a). The high activity of the amorphous Fe catalyst could be attributed to the fact that the amorphous catalyst has a much greater structural distortion and therefore a much higher concentration of active sites for the catalytic reaction than its crystalline counterpart pre-reduced by $NaBH_4$ (Fig. 3b) [45].

Table 1
Catalytic activities of noble metal-based catalysts for the generation of hydrogen from aqueous AB.

Catalyst	Average metal particle size (nm)	Maximum H_2/AB molar ratio	Time to completion (min)	Activation energy (kJ mol^{-1})	Catalyst/AB molar ratio	Ref.
20 wt% Pt/C, 40 wt% Pt/C, PtO_2, Pt black		3.0	≤10		0.018	[30]
K_2PtCl_4		3.0	≈18		0.018	[30]
Rh[(1,5-COD)(μ-Cl)]$_2$		≈2.5	≈10		0.018	[30]
Pd black		≈2.7	250		0.018	[30]
K_2PtCl_6				87		[32]
Ru/γ-Al_2O_3	1.8	3.0	3	23	0.018	[33]
Rh/γ-Al_2O_3	2.5	3.0	1.3	21	0.018	[33]
Pd/γ-Al_2O_3	3.6	2.9	120		0.018	[33]
Pt/γ-Al_2O_3	1.5	3.0	0.75	21	0.018	[33]
Au/γ-Al_2O_3	2.6	1.9	610		0.018	[33]
Pt/SiO_2	5.1	3.0	3		0.018	[33]
Ru/C				76 or 60.4		[36,37]
Zeolite stabilized Rh(0)	Small	3.0	8	67	0.004	[42]
PSSA-*co*-MA stabilized Ru(0)				54		[40]
PSSA-*co*-MA stabilized Pd(0)				44		[40]
Laurate stabilized Rh(0)	5.2 ± 2.7	3.0	6		0.0025	[38]
Laurate stabilized Ru(0)	2.6 ± 1.2	3.0	22	47	0.00125	[39]
Laurate stabilized Ru(0)	2.6 ± 1.2	3.0	8	47	0.005	[39]
Zeolite stabilized Pd(0)		3.0		56		[43]

There are quite a few reports on various Ni-based catalysts towards hydrolysis of AB due to the special preference of researchers. Experimental investigations have found that Ni NPs with or without capping agent possess high catalytic activities for H_2 generation from aqueous solution of AB. However, the catalytic activities of the Ni NPs almost remained even after 240 h when water-soluble starch was employed as the "green" capping agent for Ni NPs. In contrast, the catalytic activities of Ni NPs without starch decreased seriously in the course of the lifetime tests. The XPS results demonstrate that starch can successfully keep the Ni NPs in aqueous solution from the oxidation in air, resulting in the retainable activity [46]. Likewise, the PVP stabilized nickel catalyst can keep high activity for hydrolysis of AB to generate a stoichiometric amount of hydrogen with the cycle number up to 5, while the reaction rate in the presence of the bare nickel catalyst decreases when additional cycles are performed. The study indicate that PVP may prevent agglomeration and crystallization of nickel NPs, resulting in higher durability of PVP stabilized Ni than the bare Ni catalyst [47]. The $Fe_{1-x}Ni_x$ (x = 0, 0.3, 0.4, 0.5, 0.7 and 1) nano-alloys were also *in situ* prepared by a facile method for H_2 generation from the aqueous AB solution under ambient atmosphere at room temperature [48]. The obtained nano-alloys, especially for $Fe_{0.5}Ni_{0.5}$, have very high catalytic activity and can be readily magnetically separated for further recycling and remain the same high activity even after 5 catalytic cycles under ambient conditions. The Ni@SiO_2 nanospheres prepared with reversed micelle method were found to have higher catalytic activity for hydrolysis of AB to generate stoichiometric amount of H_2 compared to the Ni/SiO_2 nanosphere and Ni/commercial SiO_2 catalysts, which were synthesized by depositing Ni NPs on SiO_2 nanospheres and commercial SiO_2, respectively, with impregnation method [49]. Li and co-workers employed a Ni-based metal-organic framework (MOF) as precursor for preparing a mixture of Ni NPs with undegradated Ni-MOF reduced by AB in methanol. The mixture exhibits a high catalytic activity for complete hydrogen generation from aqueous AB solution at 25 °C in air [50]. Monodisperse nickel NPs were synthesized by the reduction of Ni(acac)$_2$ with borane tributylamine (BTB) in the presence of oleylamine (OAm) and oleic acid (OA). The as-synthesized Ni NPs supported on the Ketjen carbon support were reported to exhibit high catalytic activity in hydrogen generation from the hydrolysis of the AB even at low catalyst and substrate concentrations at room temperature [51].

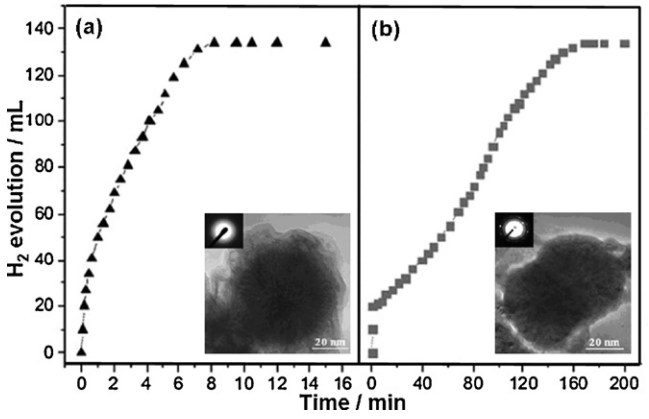

Fig. 3. Hydrogen generation by hydrolysis of aqueous AB (0.16 M, 10 mL) in the presence of (a) *in situ* synthesized Fe catalysts and (b) the pre-synthesized (Fe/AB = 0.12) at room temperature under argon. Inset: TEM micrographs and the corresponding SAED patterns of the Fe NPs [45]. Scale bar: 20 nm.

Copper NPs have been prepared by the solvated metal atom dispersion (SMAD) method. Oxidation of the SMAD prepared copper colloids led to Cu@Cu_2O core shell structures (7.7 ± 1.8 nm) or Cu_2O NPs, depending on the different reaction conditions. The Cu@Cu_2O core shell and Cu_2O NPs show better activities than pure Cu NPs for the generation of hydrogen in the AB hydrolysis reaction [52]. Zeolite confined Cu NPs were prepared by the ion-exchange of Cu^{2+} ions with the extra framework Na^+ ions in zeolite-Y followed by reduction of the Cu^{2+} ions within the cavities of zeolite with $NaBH_4$ in aqueous solution. Zeolite confined Cu NPs are active in the hydrolysis of AB with an average TOF value of 46.5 h^{-1} and provide 1300 turnovers in the catalytic hydrolytic dehydrogenation of AB [53].

Compared to Ni- and Cu-based NPs, Co analogs seem to be more active toward hydrolysis reaction of AB [54]. The amorphous and well dispersed Co NPs (less than 10 nm) were *in situ* prepared without additional dispersing agent in aqueous solution at room temperature by our group recently. The as-synthesized Co NPs have high catalytic activity (1116 L mol^{-1} min^{-1}) and excellent recycling performance (without activity loss in five recycles) for the hydrogen generation from AB aqueous solution under ambient conditions [55]. Demirci and Miele investigated $CoCl_2$-catalyzed hydrolysis of AB with the concern of improving the effective gravimetric hydrogen storage capacity (GHSC) of the system AB-H_2O by systematically changing the water amount [56]. They obtained effective GHSC of 7.8 wt% at 25 °C and hydrogen generation rate

Table 2
Catalytic activities of non-noble metal catalysts for the generation of hydrogen from aqueous AB.

Catalyst	Crystallinity	Average metal particle size (nm)	Maximum H_2/AB molar ratio	Time to completion (min)	Activation energy (kJ mol^{-1})	Catalyst/AB molar ratio	Ref.
10 wt% Co/γ-Al_2O_3	Crystalline	13	2.9	70	62	0.018	[44]
10 wt% Co/SiO_2	Crystalline	12	2.9	70		0.018	[44]
10 wt% Co/C	Crystalline	2.5	2.9	55		0.018	[44]
10 wt% Ni/γ-Al_2O_3	Crystalline	3.8	2.9	65		0.018	[44]
10 wt% Cu/γ-Al_2O_3	Crystalline	17	2.9	590		0.018	[44]
10 wt% Fe/γ-Al_2O_3	Crystalline	16	0			0.018	[44]
Fe	Amorphous	60	3	8		0.12	[45]
Fe	Crystalline	<100	~3	160		0.12	[45]
Ni in starch	Amorphous	<10	3	6		0.1	[46]
Bare Ni NPs	Amorphous		2.8	11		0.1	[47]
PVP-Ni NPs	Amorphous		2.7	9		0.1	[47]
$Fe_{0.5}Ni_{0.5}$	Amorphous	3	3	2.2		0.12	[48]
Ni@SiO_2	Amorphous	<ca. 3	~3	22		0.05	[49]
Ni/SiO_2 nanosphere	Amorphous		2.0	76		0.05	[49]
Ni/commercial SiO_2	Amorphous		1.9	120		0.05	[49]
MOF-based Ni NPs	Amorphous	~100	3	5		0.10	[50]
Ni/C	Crystalline	3.2	3.0	~11	28 ± 2	0.0425	[51]
Zeolite stabilized Cu			3.0	~120	52 ± 2	0.0133	[53]
Co	Amorphous	<10	3	1.7		0.04	[55]
PVP stabilized Co					46 ± 2	0.015	[57]
Ni hollow sphere	Crystalline		0.6	120		~0.025	[60]
Ni@SiO_2 nanosphere			2.7	23		0.065	[61]

of 21 ml(H_2) min^{-1}. Furthermore, although the water excess and the temperature increase favor higher hydrogen generation rates (HGRs), both of which have detrimental effects on the effective GHSC. Metin and Özkar prepared PVP stabilized Co NPs for hydrolysis of AB and found the catalyst was highly active. Kinetic studies show that the catalytic hydrolysis of AB is of first order with respect to catalyst and substrate concentration in aqueous medium [57]. Shul et al. combined Ni, Cu and Co with variable compositions and prepared the ternary composite with facile $NaBH_4$ reduction. Among all the catalysts with various proportions of Ni/Cu/Co investigated, $Ni_{60}Co_{20}Cu_{20}$/ACF (active carbon fiber) showed the highest hydrogen release rate from AB aqueous solution (9.0 L min^{-1} g^{-1}). Theoretical amounts of hydrogen were released from AB solution with the developed catalyst until it was deactivated [58]. Table 2 shows a part of non-noble metal-based catalysts for hydrogen generation from aqueous AB.

It is worthy to note that incomplete hydrogen release happens to some catalysts, as shown in Tables 1 and 2. The reason for incomplete dehydrogenation catalyzed over these catalysts is possibly owing to side reaction beside hydrolysis of ammonia borane. The possible side reaction is dehydrogenation of ammonia borane as the following Eqs. (2) and (3) [21,59]. Obviously, less amount of hydrogen is generated via the Eqs. (2) and (3) than via hydrolysis of ammonia borane (Eq. (1)) from the same amount of starting ammonia borane.

$$NH_3BH_3 \rightarrow H_2NBH_2 + H_2 \quad (2)$$

$$H_2NBH_2 \rightarrow HNBH + H_2 \quad (3)$$

3.3. Synergistic effects of noble and non-noble metal catalysts

Bimetallic catalysts usually show enhanced catalytic performance in comparison to their monometallic counterparts. Since the properties of the catalyst surfaces are closely related with the catalytic activities, the precise modification of the noble metal-based catalyst surface by introducing a second metal, especially a non-noble metal component, or changing the morphology could facilitate the improvement of the catalytic properties. Submicrometer-sized $Ni_{1-x}Pt_x$ (x = 0–0.12) hollow spheres prepared by a poly(styrene-*co*-methacrylic acid) (PSA)-assisted template route exhibit favorable catalytic activities in the hydrolysis of AB with rapid kinetics [60]. Similarly, Pt_xNi_{1-x} NPs of 2–4 nm through a redox replacement reaction with a reverse micromulsion technique were reported recently. Among the catalysts with different Pt/Ni ratio, $Pt_{0.65}Ni_{0.35}$ displays the highest catalytic performance with a high hydrogen release rate of 4784.7 mL min^{-1} g^{-1} and a low activation energy of 39.0 kJ mol^{-1} [62]. Yang and coworkers investigated two types of Pt- and Ni-based alloy NPs with 5–20 nm sizes for hydrogen generation from aqueous AB [63]. The experimental results demonstrated that hydrogen release rates from most of the Ni alloy catalysts exhibited greatly enhanced catalytic activities than pure Ni catalyst. Especially, bimetallic NiAg alloy catalyst was found to be highly active and efficient for hydrogen release from AB hydrolysis at room temperature showing a stable hydrogen yield at H_2/AB = 2.9 (molar ratio) [63]. Liu et al. reported hollow metallic nickel spheres with an average diameter of 1.8 μm synthesized via a decomposition and H_2 reduction route by using hollow nickel hydroxide spheres as precursors [64]. Various bimetallic (Ni/Au, Ni/Ag, Ni/Pt, and Ni/Pd) and noble metal (Pt and Pd) hollow metallic spheres have also been obtained via a replacement reaction route by using hollow metallic nickel spheres as sacrificial templates, among which the Ni/Pt hollow bimetallic spheres exhibit synergistic improvement of catalytic activity in AB hydrolysis reaction in contrast to the monometallic Ni and Pt counterparts [64]. Recently, we have prepared Ni, Au, and Au-Ni NPs with small diameters (3-4 nm for Au-Ni NPs) within silica nanospheres (around 15 nm) by using $Au(en)_2Cl_3$ and $Ni(NH_3)_6Cl_2$ as precursors in a NP-5/cyclohexane reversed-micelle system, and by *in situ* reduction in an aqueous solution of $NaBH_4$/AB [61]. The Ni NPs in Ni@SiO_2 remain small whereas quite a few Au NPs in Au@SiO_2 readily aggregate, possibly due to their different surface energies. The Ni stabilizes Au NPs to give Au–Ni NPs that remain small and form very few agglomerations. Compared with monometallic Au@SiO_2 and Ni@SiO_2, the Au–Ni@SiO_2 catalyst exhibits superior performances in the hydrolytic dehydrogenation of AB in many aspects: (1) Au–Ni@SiO_2 presents the best activity in hydrogen generation, giving the highest hydrogen productivity in the shortest time of all three catalysts, whereas Au@SiO_2 shows the lowest activity. (2) The hydrogen productivity of Ni@SiO_2 is greatly reduced after the first run, whereas it remains almost constant even after over 10 runs with the Au–Ni@SiO_2 catalyst. (3) As-synthesized Ni@SiO_2 is almost inactive for hydrogen generation in the absence of $NaBH_4$, whereas it has no great influence on the catalytic activity of Au–Ni@SiO_2 either in its presence or absence. Simply, the syner-

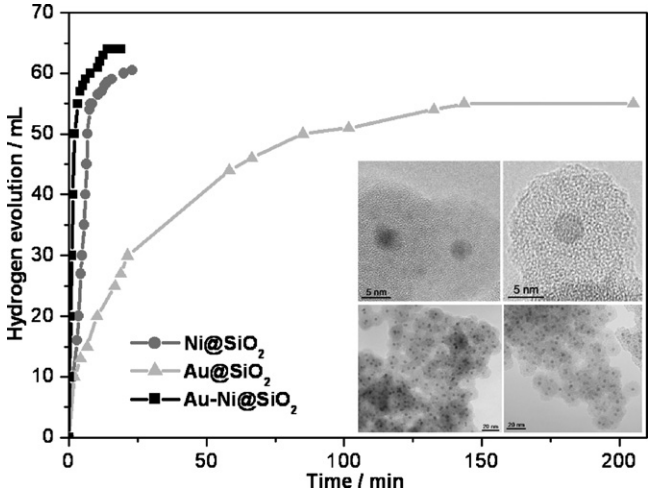

Fig. 4. Hydrogen generation by hydrolysis of ammonia borane (AB, 0.152 M, 5 mL) in the presence of as-synthesized $Ni@SiO_2$, $Au@SiO_2$ and $Au–Ni@SiO_2$ catalysts (Au/AB = 0.019, Ni/AB = 0.065) at 18 °C in air (inset: TEM images for $Au–Ni@SiO_2$ nanospheres. The scale bars are 5 nm and 20 nm, respectively, for the two upper and two bottom images).

gistic effect between Au and Ni is apparent during the generation of hydrogen: The Ni species stabilizes the Au NPs and the existence of Au helps to improve the catalytic activity and durability of the Ni NPs (Fig. 4) [61].

In addition to bimetallic alloy NPs, bimetallic core–shell NPs have attracted much attention owing to their unique properties and potential applications compared to monometallic counterparts and alloys. Mostly recently, our group successfully prepared magnetically recyclable Au@Co core–shell NPs by a rational and general strategy through the one-step seeding-growth route with AB as the reducing agent under ambient conditions within a few minutes [65]. On the basis of the difference in reduction potentials of $E^0_{Co^{2+}/Co}$ (−0.28 eV vs. SHE) and $E^0_{Au^{2+}/Au}$ (+0.93 eV vs. SHE), the core Au NPs can be formed firstly and served as the *in situ* seeds for the successive catalytic reduction, resulting in the growth of outer Co NPs as a shell in the AB aqueous solution although the Au^{3+} and Co^{2+} precursors were added simultaneously. Unexpectedly, compared to the monometallic and alloy counterparts, the resultant magnetically recyclable Au@Co NPs displayed excellent catalytic activity and long-term stability towards hydrolytic dehydrogenation of aqueous AB under ambient conditions (Fig. 5) [65].

3.4. Others

In recent two years, some researchers have developed B-contained nanocomposites, thin films and foams and found they have considerable activities toward hydrolysis of AB. Patel et al. have proved that nanoparticle-assembled Co–B thin films synthesized by pulsed laser deposition (PLD) act as efficient catalysts for hydrolysis of AB to produce hydrogen. The comparison was made with the same amount of amorphous Co–B powders, which exhibited a lower rate (about 1/6) of H_2 generation. 2.85 mol of H_2, instead of the maximum expected (3.0 equiv.), were obtained with the Co–B films at room temperature. The activation energy of the rate limiting process involved in the final hydrogen production is 34 kJ mol^{-1} and the H_2 generation rate is similar to that reported for Pt/Al_2O_3 [66]. Magnetically recyclable Co–B hollow nanospindles prepared by using poly(styrene-comethacrylic acid) nanospindles as scarified templates were used for hydrogen generation from hydrolysis of AB. Results showed that the activity of Co–B hollow nanospindles was much higher than that of regular Co–B prepared without templates. The Co–B hollow nanospindles also have good reusability (the activity has no obvious decrease after seven cycles) in the application due to their unique magnetic properties. The authors attributed the favorable activity to the large specific surface area and hollow structure [67]. Wang et al. have prepared a cost-effective Co–Mo–B alloy/Ni foam catalyst by using a modified electroless plating method. After being calcined at an optimized condition (at 350 °C under Ar atmosphere for 2 h), the catalyst exhibits high and durable catalytic activity towards the hydrolysis reaction of AB at ambient temperatures. The hydrolysis of AB in the presence of Co–Mo–B/Ni foam catalyst exhibits first-order kinetics with respect to AB concentration and catalyst amount, respectively, with an apparent activation energy of 44.3 kJ mol^{-1} [68]. With a similar method, Kwon et al. synthesized Co–P/M (M = Ni or Cu) catalysts and the effects of the catalysts on the H_2 generation kinetics in AB solution as well as their cyclic behavior (durability) were investigated. The H_2 generation rate/projected area of Co–P deposited on Ni foam is much higher (4.6 times) than that of the Co–P/Cu sheet

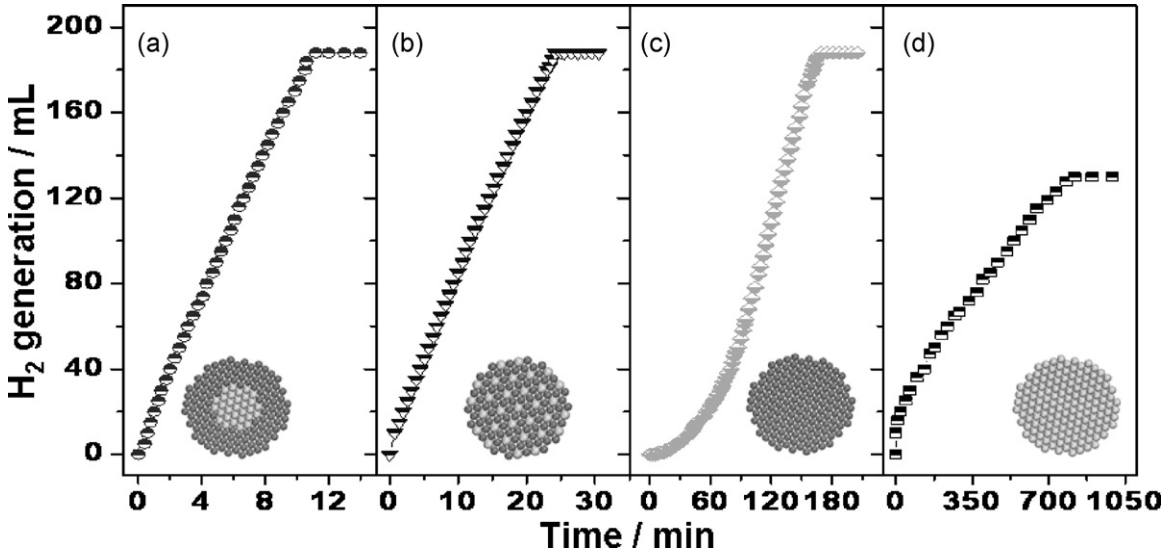

Fig. 5. Hydrogen generation from AB aqueous solution (0.26 M, 10 mL) catalyzed by (a) Au@Co, (b) Au–Co, (c) Co, and (d) Au NPs under ambient conditions. Catalyst/AB = 0.02 (molar ratio) [64].

catalyst. The activation energy for the hydrolysis of AB using the Co–P/Ni foam catalyst is 48 kJ mol^{-1} [69].

In addition to the hydrolysis of AB, similar methanolysis of AB has also been developed to generate pure hydrogen at room temperature over various catalysts (Eq. (4)), such as $RuCl_3$, $RhCl_3$, $CoCl_2$, $NiCl_2$, Pd/C, Raney Ni, PVP-stabilized Pd NPs, zeolite stabilized Rh NPs, Co–Co_2B, Ni–Ni_3B, and Co–Ni–B, etc. [25,70,71,52]. Hydrogen capacity from the above system is calculated to be about 3.9 wt%, which is lower than that from the hydrolytic system (about 7.8 wt%).

$$NH_3BH_3 + 4MeOH \rightarrow NH_4B(OMe)_4 + 3H_2 \quad (4)$$

Recently, two methods involving water but no catalysts have been developed for releasing hydrogen from AB [72–74]. One is based on combustion of AB mixtures with aluminum powder and gelled water. It was experimentally shown that these mixtures, upon ignition, exhibit self-sustained combustion with hydrogen release from both AB and water, 7.7 wt% H_2 in total. The other method involves external heating of aqueous AB solutions to ~120 °C or higher under argon pressure to avoid water boiling. Experiments show that heating aqueous AB solutions to temperatures 117–170 °C releases 3 equiv. of hydrogen per mole AB, where 2–2.1 equiv. originate from AB and 0.9–1 equiv. from water.

4. Conclusions and outlook

In conclusion, hydrolysis of AB presents a high hydrogen capacity up to 7.8 wt% of the starting materials, AB and H_2O, which shows to be a promising hydrogen storage system. The AB aqueous solution is stable in inert atmosphere and does not need any additional stabilizer. A portable hydrogen generation system is expected to be established on the basis of the metal-catalyzed dissociation and hydrolysis of AB. Thanks to recent research efforts, the reaction proceeds under ambient conditions with rapid kinetics in the presence of suitable catalysts; not only noble metal but also many highly active non-noble metal-based catalysts have been developed. In addition, the apparatus for AB hydrolysis reaction could be self-assembled and easily available, and the characterizations of the reaction products and kinetics are also readily performed. Similar to catalytic CO oxidation reaction [75–77], the convenience of performing AB hydrolysis reaction makes it be applicable and has already been used as a test (model) reaction for examining the catalytic activity of new materials [64].

It is worthy to note that there could be some ammonia release during the H_2 generation from hydrolysis of AB, especially in the cases of high AB concentrations [25,56]. The released ammonia should be removed, for example, by absorbents, before introducing into fuel cells to avoid its damage. For practical applications of AB hydrolytic dehydrogenation in portable electric devices, further experimental and theoretical studies for pending limitations, such as (i) how to break the strong B–O bonds formed during the H_2 generation to recycle the end products and (ii) how to reduce the catalyst deactivation, etc., are highly desired to overcome the high material cost issue.

It is noticed that further significant developments have been achieved for liquid-phase chemical hydrogen storage recently. It is reported that hydrous hydrazine N_2H_4 can be selectively decomposed to H_2 and N_2 with suitable catalysts, such as RhNi, PtNi and IrNi bimetallic catalysts, at room temperature [13,22,78–80], while hydrazine boranes such as $N_2H_4BH_3$ and $N_2H_4(BH_3)_2$ can release hydrogen via thermolysis [81]. It is highly expected that a catalyst, such as RhNi, PtNi or IrNi bimetallic catalyst, with catalytic activity for both reactions of AB hydrolysis and hydrous hydrazine decomposition might exhibit good activity and H_2 selectivity for the hydrogen generation from hydrazine boranes via both hydrolysis of the BH_3 group and complete decomposition of the hydrazine group, which might give higher hydrogen storage capacity, for example, 12.3 wt% and 15.3 wt% for the $N_2H_4BH_3$ and $N_2H_4(BH_3)_2$ systems, respectively, according to Eqs. (5) and (6).

$$N_2H_4BH_3 + 2H_2O \rightarrow N_2 + HBO_2 + 5H_2 \quad (5)$$

$$N_2H_4(BH_3)_2 + 4H_2O \rightarrow N_2 + 2HBO_2 + 8H_2 \quad (6)$$

We are looking forward to new breakthrough towards the use of ammonia borane and its derivatives as chemical hydrogen storage materials and the overcoming of the limitations mentioned above in near future.

Acknowledgements

The authors gratefully acknowledge AIST and JSPS for financial support. H.L. J. thanks JSPS for a postdoctoral fellowship.

References

[1] S. Satyapal, J. Petrovic, C. Read, G. Thomas, G. Ordaz, Catal. Today 120 (2007) 246–256.
[2] U.S. Department of Energy, Hydrogen Program, http://www.hydrogen.energy.gov/.
[3] L. Schlapbach, A. Züttel, Nature 414 (2001) 353–358.
[4] S. Orimo, Y. Nakamori, J.R. Eliseo, A. Züttel, C.M. Jensen, Chem. Rev. 107 (2007) 4111–4132.
[5] M. Jordá-Beneyto, F. Suárez-García, D. Lozano-Castelló, D. Cazorla-Amorós, A. Linares-Solano, Carbon 45 (2007) 293–303.
[6] H.W. Langmi, G.S. McGrady, Coord. Chem. Rev. 251 (2007) 925–935.
[7] L.J. Murray, M. Dincă, J.R. Long, Chem. Soc. Rev. 38 (2009) 1294–1314.
[8] G.A. Deluga, J.R. Salge, L.D. Schmidt, X.E. Verykios, Science 303 (2004) 993–997.
[9] P. Makowski, A. Thomas, P. Kuhn, F. Goettmann, Energy Environ. Sci. 2 (2009) 480–490.
[10] P. Chen, Z.T. Xiong, J.Z. Luo, J.Y. Lin, K.L. Tan, Nature 420 (2002) 302–304.
[11] Y. Kojima, Y. Kawai, M. Kimbara, H. Nakanishi, S. Matsumoto, Int. J. Hydrogen Energy 29 (2004) 1213–1217.
[12] C.W. Hamilton, R.T. Baker, A. Staubitz, I. Manners, Chem. Soc. Rev. 38 (2009) 279–293.
[13] S.K. Singh, X.B. Zhang, Q. Xu, J. Am. Chem. Soc. 131 (2009) 9894–9895.
[14] U.B. Demirci, F. Garina, J. Mol. Catal. A: Chem. 279 (2008) 57–62.
[15] A. Gutowska, L. Li, Y. Shin, C.M. Wang, X.S. Li, J.C. Linehan, R.S. Smith, B.D. Kay, B. Schmid, W. Shaw, M. Gutowski, T. Autrey, Angew. Chem. Int. Ed. 44 (2005) 3578–3582.
[16] Z. Li, G. Zhu, G. Lu, S. Qiu, X. Yao, J. Am. Chem. Soc. 132 (2010) 1490–1491.
[17] F.H. Stephens, R.T. Baker, M.H. Matus, D.J. Grant, D.A. Dixon, Angew. Chem. Int. Ed. 46 (2007) 746–749.
[18] P. Wang, X.D. Kang, Dalton Trans. 40 (2008) 5400–5413.
[19] T. Umegaki, J.M. Yan, X.B. Zhang, H. Shioyama, N. Kuriyama, Q. Xu, Int. J. Hydrogen Energy 34 (2009) 2303–2311.
[20] Q. Xu, M. Chandra, J. Alloys Compd. 446 (2007) 729–732.
[21] F.H. Stephens, V. Pons, R.T. Baker, Dalton Trans. 25 (2007) 2613–2626.
[22] H.L. Jiang, S.K. Singh, J.M. Yan, X.B. Zhang, Q. Xu, ChemSusChem 3 (2010) 541–549.
[23] T.B. Marder, Angew. Chem. Int. Ed. 46 (2007) 8116–8118.
[24] U.B. Demirci, P. Miele, Energy Environ. Sci. 2 (2009) 627–637.
[25] P.V. Ramachandran, P.D. Gagare, Inorg. Chem. 46 (2007) 7810–7817.
[26] M.E. Bluhm, M.G. Bradley, R. Butterick III, U. Kusari, L.G. Sneddon, J. Am. Chem. Soc. 128 (2006) 7748–7749.
[27] L. Li, X. Yao, C.H. Sun, A.J. Du, L.N. Cheng, Z.H. Zhu, C.Z. Yu, J. Zou, S.C. Smith, P. Wang, H.M. Cheng, R.L. Frost, G.Q.M. Lu, Adv. Funct. Mater. 19 (2009) 265–271.
[28] Z.T. Xiong, C.K. Yong, G.T. Wu, P. Chen, W. Shaw, A. Karkamkar, T. Autrey, M.O. Jones, S.R. Johnson, P.P. Edwards, W.I.F. David, Nat. Mater. 7 (2008) 138–141.
[29] H.V.K. Diyabalanage, R.P. Shrestha, T.A. Semelsberger, B.L. Scott, M.E. Bowden, B.L. Davis, A.K. Burrell, Angew. Chem. Int. Ed. 46 (2007) 8995–8997.
[30] M. Chandra, Q. Xu, J. Power Sources 156 (2006) 190–194.
[31] M. Chandra, Q. Xu, J. Power Sources 159 (2006) 855–860.
[32] N. Mohajeri, A. T-Raissi, O. Adebiyi, J. Power Sources 167 (2007) 482–485.
[33] M. Chandra, Q. Xu, J. Power Sources 168 (2007) 135–142.
[34] T.J. Clark, G.R. Whittell, I. Manners, Inorg. Chem. 46 (2007) 7522–7527.
[35] V.I. Simagina, P.A. Storozhenko, O.V. Netskina, O.V. Komova, G.V. Odegova, Y.V. Larichev, A.V. Ishchenko, A.M. Ozerova, Catal. Today 138 (2008) 253–259.
[36] S. Basu, A. Brockman, P. Gagare, Y. Zheng, P.V. Ramachandran, W.N. Delgass, J.P. Gore, J. Power Sources 188 (2009) 238–243.
[37] S. Basu, Y. Zheng, A. Varma, W.N. Delgass, J.P. Gore, J. Power Sources 195 (2010) 1957–1963.
[38] F. Durap, M. Zahmakıran, S. Özkar, Appl. Catal. A: Gen. 369 (2009) 53–59.
[39] F. Durap, M. Zahmakıran, S. Özkar, Int. J. Hydrogen Energy 34 (2009) 7223–7230.
[40] Ö. Metin, S. Sxahin, S. Özkar, Int. J. Hydrogen Energy 34 (2009) 6304–6313.
[41] S. Özkar, Appl. Surf. Sci. 256 (2009) 1272–1277.

[42] M. Zahmakıran, S. Özkar, Appl. Catal. B: Environ. 89 (2009) 104–110.
[43] F. Durap, S. Özkar, Int. J. Hydrogen Energy 35 (2010) 1305–1312.
[44] Q. Xu, M. Chandra, J. Power Sources 163 (2006) 364–370.
[45] J.M. Yan, X.B. Zhang, S. Han, H. Shioyama, Q. Xu, Angew. Chem. Int. Ed. 47 (2008) 2287–2289.
[46] J.M. Yan, X.B. Zhang, S. Han, H. Shioyama, Q. Xu, Inorg. Chem. 48 (2009) 7389–7393.
[47] T. Umegaki, J.M. Yan, X.B. Zhang, H. Shioyama, N. Kuriyama, Q. Xu, Int. J. Hydrogen Energy 34 (2009) 3816–3822.
[48] J.M. Yan, X.B. Zhang, S. Han, H. Shioyama, Q. Xu, J. Power Sources 194 (2009) 478–481.
[49] T. Umegaki, J.M. Yan, X.B. Zhang, H. Shioyama, N. Kuriyama, Q. Xu, J. Power Sources 191 (2009) 209–216.
[50] Y. Li, L. Xie, Y. Li, J. Zheng, X. Li, Chem. Eur. J. 15 (2009) 8951–8954.
[51] Ö. Metin, V. Mazumder, S. Özkar, S. Sun, J. Am. Chem. Soc. 132 (2010) 1468–1469.
[52] S.B. Kalidindi, A.A. Vernekar, B.R. Jagirdar, Phys. Chem. Chem. Phys. 11 (2009) 770–775.
[53] M. Zahmakıran, F. Durap, S. Özkar, Int. J. Hydrogen Energy 35 (2010) 187–197.
[54] S.B. Kalidindi, M. Indirani, B.R. Jagirdar, Inorg. Chem. 47 (2008) 7424–7429.
[55] J.M. Yan, X.B. Zhang, H. Shioyama, Q. Xu, J. Power Sources 195 (2010) 1091–1094.
[56] U.B. Demirci, P. Miele, J. Power Sources 195 (2010) 4030–4035.
[57] Ö. Metin, S. Özkar, Energy Fuels 23 (2009) 3517–3526.
[58] J.H. Park, H.S. Kim, H.J. Kim, M.K. Han, Y.G. Shul, Res. Chem. Intermed. 34 (2008) 709–715.
[59] R.J. Keaton, J.M. Blacquiere, R.T. Baker, J. Am. Chem. Soc. 129 (2007) 1844–1845.
[60] F. Cheng, H. Ma, Y. Li, J. Chen, Inorg. Chem. 46 (2007) 788–794.
[61] H.L. Jiang, T. Umegaki, T. Akita, X.B. Zhang, M. Haruta, Q. Xu, Chem. Eur. J. 16 (2010) 3132–3137.
[62] X. Yang, F. Cheng, J. Liang, Z. Tao, J. Chen, J. Power Sources 34 (2009) 8785–8791.
[63] C.F. Yao, L. Zhuang, Y.L. Cao, X.P. Ai, H.X. Yang, Int. J. Hydrogen Energy 33 (2008) 2462–2467.
[64] R. Yi, R. Shi, G. Gao, N. Zhang, X. Cui, Y. He, X. Liu, J. Phys. Chem. C 113 (2009) 1222–1226.
[65] J.M. Yan, X.B. Zhang, T. Akita, M. Haruta, Q. Xu, J. Am. Chem. Soc. 132 (2010) 5326–5327.
[66] N. Patel, R. Fernandes, G. Guella, A. Miotello, Appl. Catal. B: Environ. 95 (2010) 137–143.
[67] D.G. Tong, X.L. Zeng, W. Chu, D. Wang, P. Wu, J. Mater. Sci. 45 (2010) 2862–2867.
[68] H.B. Dai, L.L. Gao, Y. Liang, X.D. Kang, P. Wang, J. Power Sources 195 (2010) 307–312.
[69] K.S. Eom, M.J. Kim, R.H. Kim, D.H. Nam, H.S. Kwon, J. Power Sources 195 (2010) 2830–2834.
[70] H. Erdoğan, Ö. Metin, S. Özkar, Phys. Chem. Chem. Phys. 11 (2009) 10519–10525.
[71] S. Çalışkan, M. Zahmakıran, S. Özkar, Appl. Catal. B: Environ. 93 (2010) 387–394.
[72] M. Diwan, V. Diakov1, E. Shafirovich, A. Varma, Int. J. Hydrogen Energy 33 (2008) 1135–1141.
[73] M. Diwan, D. Hanna, A. Varma, Int. J. Hydrogen Energy 35 (2010) 577–584.
[74] S. Basu, M. Diwan, M.G. Abiad, Y. Zheng, O.H. Campanella, A. Varma, Int. J. Hydrogen Energy 35 (2010) 2063–2072.
[75] M. Haruta, T. Kobayashi, H. Sano, N. Yamada, Chem. Lett. 16 (1987) 405–408.
[76] M. Haruta, N. Yamada, T. Kobayashi, S. Iijima, J. Catal. 115 (1989) 301–309.
[77] H.L. Jiang, B. Liu, T. Akita, M. Haruta, H. Sakurai, Q. Xu, J. Am. Chem. Soc. 131 (2009) 11302–11303.
[78] S.K. Singh, Q. Xu, J. Am. Chem. Soc. 131 (2009) 18032–18033.
[79] S.K. Singh, Q. Xu, Inorg. Chem. 49 (2010) 6148–6152.
[80] S.K. Singh, Q. Xu, Chem. Commun. 46 (2010) 6545–6547.
[81] T. Hügle, M.F. Kühnel, D. Lentz, J. Am. Chem. Soc. 131 (2009) 7444–7446.